Biochemistry

Article

Cite This: Biochemistry 2018, 57, 1462−1474

pubs.acs.org/biochemistry

Isoindole Linkages Provide a Pathway for DOPAL-Mediated Cross-Linking of α-Synuclein

Jonathan W. Werner-Allen,[†] Sarah Monti,[‡] Jenna F. DuMond,[‡] Rodney L. Levine,*[,‡] and Ad Bax*[,†]

[†]Laboratory of Chemical Physics, National Institute of Diabetes and Digestive and Kidney Diseases, and [‡]Laboratory of Biochemistry, National Heart, Lung, and Blood Institute, National Institutes of Health, Bethesda, Maryland 20892, United States

Supporting Information

ABSTRACT: 3,4-Dihydroxyphenylacetaldehyde (DOPAL) is a toxic and reactive product of dopamine catabolism. In the catecholaldehyde hypothesis for Parkinson's disease, it is a critical driver of the selective loss of dopaminergic neurons that characterizes the disease. DOPAL also cross-links α-synuclein, the main component of Lewy bodies, which are a pathological hallmark of the disease. We previously described the initial adduct formed in reactions between DOPAL and α-synuclein, a dicatechol pyrrole lysine (DCPL). Here, we examine the chemical basis for DOPAL-based cross-linking. We find that autoxidation of DCPL's catechol rings spurs its decomposition, yielding an intermediate dicatechol isoindole lysine (DCIL) product formed by an intramolecular reaction of the two catechol rings to give an unstable tetracyclic structure. DCIL then reacts with a second DCIL to give a dimeric, di-DCIL. This product is formed by an intermolecular carbon-carbon bond between the isoindole rings of the two DCILs that generates two structurally nonequivalent and separable atropisomers. Using α-synuclein, we demonstrate that the DOPAL-catalyzed formation of oligomers can be separated into two steps. The initial adduct formation occurs robustly within an hour, with DCPL as the main product, and the second step cross-links α-synuclein molecules. Exploiting this two-stage reaction, we use an isotopic labeling approach to show the predominant cross-linking mechanism is an interadduct reaction. Finally, we confirm that a mass consistent with a di-DCIL linkage can be observed in dimeric α-synuclein by mass spectrometry. Our work elucidates previously unknown pathways of catechol-based oxidative protein damage and will facilitate efforts to detect DOPAL-based cross-links in disease-state neurons.

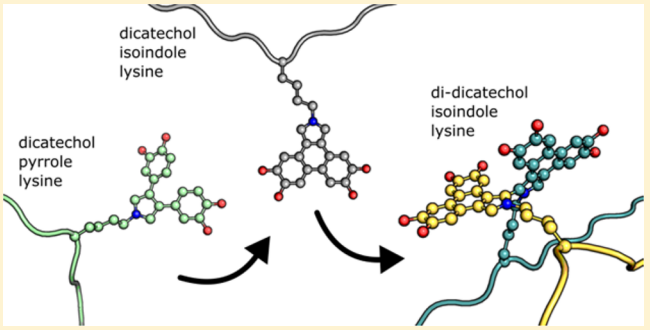

INTRODUCTION

Parkinson's disease (PD) is a progressive neurological disorder that remains incurable. The catecholaldehyde hypothesis seeks to link the two pathological hallmarks of PD, the selective loss of dopaminergic neurons in the substantia nigra and the appearance in those neurons of proteinaceous aggregates called Lewy bodies, through the neuronal metabolite 3,4-dihydroxyphenylacetaldehyde (DOPAL).[1,2] DOPAL is the product of monoamine oxidase action on dopamine and is the first and obligate intermediate along a catabolic pathway that clears the neurotransmitter from the cytosol.[3] DOPAL is toxic to cultured neurons when its levels are increased either by exogenous administration or by disrupting cellular dopamine metabolism and vesicular sequestration.[4,5] It is also toxic in vivo, at far lower levels than dopamine or its other metabolites, and leads to a selective loss of dopaminergic neurons analogous to PD.[6] DOPAL is highly reactive as well, owing to its unique chemical structure that contains a catechol ring, which is prone to oxidation, and an aldehyde, a functional group known to form covalent adducts with nucleophilic groups of macromolecules.[7] The reactivity of DOPAL's aldehyde is activated by the oxidative decomposition of its catechol group in a chain reaction catalyzed by the superoxide radical,[8,9] a reactive oxygen species and the main product of impaired mitochondrial respiration.

Other lines of evidence connect aberrant DOPAL levels to PD. DOPAL:dopamine ratios are elevated in PD brains,[10] and this may be due in part to impaired processing by aldehyde dehydrogenase (ALDH), which converts DOPAL's aldehyde group to a carboxylic acid in the next step of dopamine catabolism. Differential expression of ALDH among dopaminergic neuron subpopulations is correlated with their susceptibility to degeneration in PD,[11] and ALDH expression is downregulated in PD brains.[12] ALDH knockout mice have increased DOPAL levels and develop neurodegeneration and age-dependent motor dysfunction.[13] ALDH inhibitors also cause DOPAL accumulation, and environmental exposure to them is associated with increased PD risk.[14−16]

PD etiology is also known to involve the neuronal protein α-synuclein. α-Synuclein is the main component of Lewy bodies, and mutations or multiplications of its gene cause early onset forms of the disease.[17] α-Synuclein has 140 residues, is

Received: November 16, 2017
Revised: January 31, 2018
Published: February 2, 2018

DOI: 10.1021/acs.biochem.7b01164
Biochemistry 2018, 57, 1462−1474

intrinsically disordered, and transiently binds to negatively charged lipid membranes through an amphipathic α-helix formed by the seven imperfect 11-residue repeats of its N-terminal domain.[18] The function of α-synuclein is not established although there is evidence that it helps maintain a proper supply of synaptic vesicles and may also act as an antioxidant.[19−23] Despite significant research, it remains unclear what triggers α-synuclein aggregation in the disease state, which aggregate forms are responsible for neurotoxicity, and how they cause neurodegeneration.[24] α-Synuclein forms regular amyloid fibrils in vitro that are morphologically similar to Lewy body aggregates.[25] However, α-synuclein also forms covalent dimers and other lower order oligomers in the diseased brains of humans and animal models,[24] and increasing evidence, including the higher toxicity of small, prefibrillar aggregates, suggests that lower order oligomers are the pathologically relevant species.[26−28] Reactive endogenous small molecules and environmental toxins are known to promote covalent α-synuclein cross-linking, and their potential to nucleate and/or stabilize toxic oligomeric species has sparked recent efforts to define their roles in PD.[2,14,29−31]

DOPAL is one such compound and is localized to dopaminergic neurons, which are uniquely susceptible to degeneration in PD despite the abundant expression of α-synuclein throughout the brain. Increased intracellular DOPAL levels promote the formation of small α-synuclein oligomers in cultured cells and in vivo,[32−34] and DOPAL also potently cross-links α-synuclein in vitro,[8,32−35] in a reaction that is stimulated by superoxide,[8,9] a key mediator of oxidative stress. Although DOPAL reactivity has become the focus of increasing interest,[34−37] the chemical basis of its cross-linking ability remains unknown. Here, we study DOPAL cross-linking in vitro, describing an unexpected reaction pathway that originates with dicatechol pyrrole lysine adducts, proceeds through reactive isoindole intermediates, and results in interadduct cross-links.

MATERIAL AND METHODS

Autoxidation of Dicatechol Pyrrole Lysine and Analogues. The two dicatechol pyrrole lysine (DCPL) analogues were synthesized by Angene and were received as fine powders with pale yellow color. Stocks were prepared at ∼330 mM in deuterated methanol (99.8%, Cambridge Isotope Laboratories) and stored at −80 °C. More precise concentrations of the stocks were determined by dilution to ∼100 μM concentration in PBS (KD Medical, composed of 5.6 mM Na_2HPO_4, 1.1 mM KH_2PO_4, and 154 mM NaCl) with 100 μM diethylenetriaminepentaacetic acid (DTPA), 10% D_2O, and 10 mM ascorbate to inhibit any oxidation, and comparison of integrated intensities for the acetyl methyl signals in 1D ^{1}H NMR spectra to the acetyl methyl signal in a standard sample of 100 μM N_α-acetylated lysine. The purities of both compounds were >90% as judged by 1D ^{1}H NMR spectra and liquid chromatography−mass spectrometry (LC-MS) chromatograms. DCPL was prepared and purified as described previously.[37] After elution from the reverse phase column, each DCPL preparation was divided evenly into several aliquots, which were flash frozen in liquid nitrogen and lyophilized to dryness in the dark. A single aliquot was resuspended in 600 μL of the PBS buffer with ascorbate described above, and the amount of DCPL was calculated via the integrated intensity of its acetyl methyl signal in a 1D ^{1}H NMR spectrum again with N_α-acetylated lysine used as a reference. With ascorbate present, the oxidative decay of DCPL is negligible during this measurement. To study the autoxidation of DCPL, subsequent aliquots from the same preparation were then resuspended in the PBS buffer without ascorbate in a volume adjusted to give a 100 μM starting DCPL concentration.

Autoxidations were followed at 37 °C on a 600 MHz Bruker Avance III spectrometer equipped with a *z*-axis pulsed field gradient cryogenic probe. Each 1D ^{1}H NMR spectrum was collected with 170 scans, a 2.02 s recycle delay, a 1.0 s water presaturation pulse with a field strength of 62 Hz, and a signal acquisition time of 2.0 s for a total data collection time of 15 min. Concentrations of starting compounds and oxidation products were calculated by integration of the well-resolved acetyl methyl signals and assigned to the midpoint of each measurement time.

Purification and Characterization of DCPL Autoxidation Products. Purified, lyophilized DCPL was resuspended at ∼100 μM in 5 mL of PBS with 100 μM DTPA and incubated at 37 °C in the dark. For preparations of dicatechol isoindole lysine (DCIL) and didicatechol isoindole lysine (di-DCIL), autoxidation was allowed to proceed for 23 and 90 min, respectively, at which times the amounts of desired products are at or near their maxima while the amounts of contaminants are minimized. Samples were then immediately loaded on a Zorbax 300 Å StableBond C18 column (2.1 × 50 mm, 3.5 μm particle size, Agilent). Products were separated isocratically with deionized water at a flow rate of 0.5 mL/min. Under these conditions, chromatographic separation is based on differential hydrophobic interactions between solutes and the column resin, as noted previously for other catechol-bearing compounds.[38] Fractions containing pure product were pooled, flash frozen in liquid nitrogen, and lyophilized to dryness. For di-DCIL-1 and di-DCIL-2, the number demarcations were assigned by the order of the compounds' chromatographic elution. At all points during their purification, compounds were protected from light, and care was taken to avoid unnecessary exposure to aqueous solvent to prevent oxidation. Purified, lyophilized samples were resuspended in methanol for all subsequent analyses. Like DOPAL and DCPL, DCIL and di-DCIL are very stable to further oxidation in methanol.

NMR samples of DCIL and the two di-DCILs were prepared by resuspending the purified products in deuterated methanol, and data were collected at 25 °C on a 600 MHz Bruker Avance III spectrometer equipped with a *z*-axis gradient cryogenic probe using standard experiments and parameter sets. ^{1}H and ^{13}C chemical shifts were referenced to the methanol solvent signal at 3.31 and 49.15 ppm, respectively. Carbon chemical shifts were measured from ^{1}H−^{13}C HSQC and ^{1}H−^{13}C HMBC spectra. The ^{1}H−^{13}C HMBC spectra were recorded with a long-range coupling dephasing delay of 70 ms and acquisition times of 26 and 164 ms for the ^{13}C and ^{1}H dimensions, respectively. LC-MS was performed on the purified products resuspended in protonated methanol. Chromatographic separations were carried out on a Zorbax 300 Å StableBond C18 column (1.0 × 50 mm, 3.5 μm particle size, Agilent). The solvents were water/1% formic acid and acetonitrile/1% formic acid. A gradient of acetonitrile was developed from 0 to 70% at 2%/min with a flow rate of 20 μL/min. Electrospray ionization mass spectrometry (ESI-MS) was performed on an Agilent Model 6520 accurate mass quadrupole-time-of-flight instrument. Spectra were recorded for the mass range of 125−2500 *m*/*z*. The drying gas temperature was 300 °C with a flow rate of 10 L/min and a nebulizer pressure of

DOI: 10.1021/acs.biochem.7b01164
Biochemistry 2018, 57, 1462−1474

2 bar. The voltages were capillary, 3500 V; fragmentor, 175 V; skimmer, 65 V; and octopole, 750 V. All mass spectra were analyzed using Agilent MassHunter version B.07.00.

CD and UV−vis spectra for the two di-DCILs were collected with purified samples resuspended at ∼10 μM concentration in methanol. UV−vis spectra were blanked with methanol and collected on an Agilent 8453 spectrophotometer with a 0.5 s integration time using a cuvette with a 1 cm path length. CD spectra were also blanked with methanol and collected on a Jasco J-810 spectropolarimeter with 20 scans and a 0.5 s integration time using a cuvette with a 1 cm path length. For fluorescent measurements, di-DCIL samples were solubilized in methanol at a concentration of ∼70 μM. Data were collected on a PTI QuantaMaster spectrofluorimeter using polarizers set to the magic angle (54.7°). The temperature was set to 20 °C. Excitation slits were set to 1.00 mm, and emission slits were set to 0.50 mm. Emission was monitored at 425 nm for the excitation spectra, and the samples were excited at 350 nm for the emission spectra.

Rotational energy barriers were calculated around the di-DCIL dihedral defined by the two nitrogen atoms of the isoindole rings and the two carbons of the intermolecular bond using the dihedral driver function in Chem3D (PerkinElmer). Calculations were performed with a 1° step size and energy minimization for each conformer.

Preparation and Purification of Dicatechol Pyrrole Cadaverine. N_α-Acetylated cadaverine, formally named *N*-(5-aminopentyl)acetamide, was purchased from Santa Cruz Biotechnology, and 10× stocks were prepared in PBS and stored at −20 °C. The reactions in Figure S6 were performed at 37 °C with 1.5 mM N_α-acetylated cadaverine and 2 mM DOPAL in PBS with 100 μM DTPA and 10% D_2O. Experimental parameters for the NMR data collection were identical to those described above for DCPL autoxidation, and concentrations of dicatechol pyrrole cadaverine (DCPC) were likewise calculated from integrated intensities of its acetyl methyl signal. DCPC was purified from 5 mL reactions with the same concentrations of reactants listed above and with a similar protocol to the one reported for DCPL.[37] DCPC eluted from the Zorbax 300 Å StableBond C18 column slightly later than DCPL. As with DCPL, purified DCPC was split into several equal aliquots prior to freezing and lyophilization, and one was resuspended in PBS with ascorbate to measure the amount of purified compound. DCPC autoxidation reactions were analogous to those for DCPL described earlier. For confirming its structure and measuring the chemical shifts listed in Table S3, purified DCPC was resuspended in deuterated methanol, and 2D $^1H/^{13}C$ NMR spectra were collected with standard parameters.

Protein Cross-Linking. Recombinant α-synuclein was expressed and purified as described previously.[37] The α-synuclein gene was codon optimized to prevent cysteine misincorporation,[39] and N-terminal acetylation was achieved by coexpression of the NatB acetyltransferase.[40] For $^1H/^{15}N$-labeled samples, the addition of 1 g/L of ^{15}N-labeled IsoGro (Sigma-Aldrich) to standard M9 media is required for complete acetylation.[40] DOPAL was purchased from VDM Biochemicals, and stocks were prepared in methanol and quantified as described previously.[37]

Our standard adduct-forming reactions contained 100 μM N_α-acetylated α-synuclein (Ac-αS) and 2 mM DOPAL unless indicated otherwise and were incubated at 37 °C. For the reactions in Figure S7, samples withdrawn at the indicated times were subjected to SDS-PAGE directly. In all other experiments, protein was extracted from the adduct-forming reactions by ethanol precipitation. Four volumes of ice-cold ethanol were added to each sample followed by a 10 min incubation at −20 °C and a 5 min centrifugation at 10,000*g*. The supernatant was removed, and the protein pellet was dried briefly in vacuo. Pellets were resuspended for the second cross-linking step of the reaction at the same concentration used in the adduct-forming step. $CuCl_2$ (Sigma-Aldrich) and $NaIO_4$ (Sigma-Aldrich) were added after the complete resuspension of adducted protein at 500 μM concentration from stocks in water made at 40× and 100×, respectively. $NaIO_4$ stocks were prepared immediately prior to use. All reactions were performed in PBS, except when Cu(II) was included in which case 100 mM MOPS pH 7.4 was used to avoid the formation of insoluble phosphate salts, and were kept in the dark to prevent the photodegradation of DCPL.[37] Reactions without Cu(II) also always included 100 μM DTPA to chelate any contaminating metals. SDS-PAGE was performed with 1.5 mm NuPAGE 4−12% Bis-Tris gels (Invitrogen), and gels were stained with InstantBlue (Expedeon) and imaged at 700 nm on an Odyssey scanner (LI-COR Biosciences) using the default settings.

Protein Cross-Linking with Mixed Isotopic Labeling. DOPAL adducts were formed on nonisotopically labeled Ac-αS in a reaction with 20 μM protein and 2 mM DOPAL in 40 mL of PBS with 100 μM DTPA incubated at 37 °C for 30 min. The reaction was terminated, and excess unreacted DOPAL was removed by ethanol precipitation as described above. The pellet was resuspended in 8 mL of PBS with 100 μM DTPA that contained 100 μM $^1H/^{15}N$-labeled Ac-αS and incubated at 37 °C for 4 h to form cross-links. The reaction was concentrated to a 2 mL volume in an Amicon Ultra spin filter (EMD Millipore, 10 kDa cutoff) and loaded on a 16 mm/60 cm HiLoad Superdex 75 size exclusion column (GE Healthcare) equilibrated in PBS with 100 μM DTPA. The chromatography was run at a flow rate of 1.0 mL/min with a 1 mL fraction size. Fractions containing oligomers (fractions 39−50 in Figure 7B) were pooled and 1,000× exchanged into 20 mM sodium phosphate pH 6.2 with 10% D_2O using an Amicon Ultra spin filter to yield a final NMR sample with a volume of ∼600 μL and a total protein concentration of ∼200 μM.

All NMR spectra of protein samples were collected at 15 °C on an 800 MHz Bruker Avance III spectrometer equipped with a *z*-axis pulsed field gradient cryogenic probe. 1D ^{15}N-selected/filtered spectra were collected using the pulse sequence in Figure S9A with a 200 ms ^1H acquisition time and a 1.5 s recycle delay, and the ^{15}N-selected spectrum in Figure 7C was collected with 3× the number of scans as the ^{15}N-filtered spectrum due to the expected maximal 25% incorporation of $^1H/^{15}N$-labeled protein into the oligomers. Integrals of the amide region were calculated in TopSpin 3.1 (Bruker) after baseline correction. The integral of the ^{15}N-filtered spectra was reduced by 2.2% of its ^{15}N-selected counterpart to account for the incomplete suppression of ^{15}N-labeled signals by the filter (Figure S9C). The $^1H-^{15}N$ HSQC spectra in Figure S11 were collected with a conventional pulse sequence and acquisition times in the ^{15}N and ^1H dimensions of 243 and 106 ms, respectively. In Figure S10, intensity ratios were normalized to residue Gly101, which appeared unaffected in the oligomer sample, to correct for the different protein concentrations of the oligomer and control samples.

DOI: 10.1021/acs.biochem.7b01164
Biochemistry 2018, 57, 1462−1474

Mass Spectrometry Analysis of Purified Dimeric Protein. Preparation of dimeric, DOPAL cross-linked α-synuclein followed a similar protocol to the one described above for the mixed isotopic labeling experiment. The initial adduct-forming step was performed identically. In the second step, the cross-linking reaction was set up without $^{1}H/^{15}N$-labeled Ac-αS but was otherwise the same. At the end of a 4 h incubation at 37 °C, 10 mM ascorbate was added to the reaction from freshly prepared, pH-corrected 10× stock made in PBS. The chromatography was carried out as detailed above except that 10 mM ascorbate was included in the running buffer. The oligomeric content of the chromatographic fractions was assessed with SDS-PAGE, and the fraction with the purest dimeric α-synuclein was divided into single-use aliquots and flash frozen in liquid nitrogen. Immediately before LC-MS analysis, the dimer sample was thawed and buffer-exchanged into water using Zeba spin desalting columns (Thermo Fisher, 7 kDa cutoff) following the manufacturer's protocol. Eight microliters of product was directly injected into a solvent of 90% water and 10% acetonitrile with a flow rate of 20 μL/min pumped for 5 min. ESI-MS was performed on an Agilent Model 6520 accurate mass quadrupole-time-of-flight instrument. Spectra were recorded for the mass range of 500–2500 *m*/*z*. The drying gas temperature was 350 °C with a flow rate of 10 L/min and a nebulizer pressure of 2 bar. The voltages were capillary, 3500 V; fragmentor, 235 V; skimmer, 65 V; and octopole, 750 V.

RESULTS

Catechol Rings Drive DCPL Autoxidation. Several groups have identified lysine residues as the major target of DOPAL reactivity with α-synuclein,[7,34,35,37] although there is disagreement over the chemical identity of the adduct (see Discussion). We recently reported a quantitative analysis of the products formed in reactions between DOPAL and either N_{α}-acetylated α-synuclein (Ac-αS), the physiological form of the protein, or the model reactant N_{α}-acetylated lysine by LC-MS and NMR.[37] The predominant product was a novel dicatechol pyrrole lysine (DCPL) adduct formed by the addition of two DOPAL molecules to a single lysine side chain amine and the creation of a carbon-carbon bond between their aldehyde-adjacent carbons to give a pyrrole ring (Figure 1A). The Paal–Knorr reaction pathway provides a likely mechanism for DCPL pyrrole ring formation[41] with a DOPAL quinone methide acting as a critical intermediate.[37] We noted previously that DCPL is unstable,[37] and we expected that this instability results from oxidation of its two catechol rings.[8,9] To test this idea directly, we followed the autoxidation of DCPL and two analogue compounds, which contain either monohydroxylated or phenyl rings in place of the catechols (Figure 1A), by integrated intensities of their acetyl methyl signals in 1D ^{1}H NMR spectra. When resuspended at 100 μM concentration in PBS with 100 μM DTPA to eliminate the effect of any adventitious metals and incubated at 37 °C, purified DCPL decays rapidly, with complete degradation occurring in only 30 min (Figure 1B). In contrast, both analogues are stable for hours under the same conditions, illustrating the dominant role of the catechol rings in mediating oxidative decay (Figure 1B).

DCPL Autoxidation Products Followed by NMR. To learn more about the reactivity of DCPL, we used 1D ^{1}H NMR spectra to analyze the products of its oxidative decay. In the reactions described above, the decay of the acetyl methyl signal of purified DCPL coincided with the appearance of a new

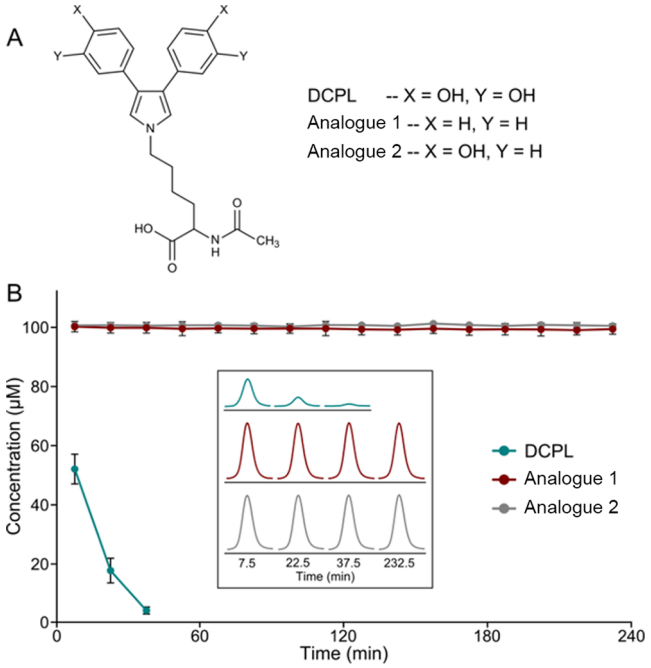

Figure 1. Catechol rings of dicatechol pyrrole lysine drive its oxidative decay. (A) Chemical structures of DCPL and synthetic analogues with the catechol rings replaced by phenyl (1) or phenol (2) rings. (B) The autoxidation of the compounds in (A) was followed at 37 °C in PBS using 1D ^{1}H NMR spectra with concentrations calculated from integrated intensities of the acetyl methyl signals. Error bars represent standard deviations from three independent samples. Whereas DCPL decays rapidly, its analogues are very stable. The inset shows the acetyl methyl ^{1}H NMR signals of DCPL (1.915 ppm), analogue 1 (1.914 ppm), and analogue 2 (1.915 ppm) that were used to calculate the concentrations in the graph at the first three and last time points of the incubation. Figure 2A provides full views of the acetyl methyl region of the ^{1}H NMR spectra for the DCPL autoxidation.

methyl signal, denoted Product A (Figure 2A). Product A is also unstable, decomposing over the course of an hour (Figure 2B), and its disappearance was accompanied by the growth of two new methyl signals, together denoted Product B (Figure 2A). The two Product B signals appear with comparable kinetics and intensities and are maximal ~70 min after the start of DCPL autoxidation (Figure 2B). The rise and decay of methyl signals for Products A and B are accompanied by two sets of aromatic signals, most of which are shifted far downfield from the DCPL signals (Figure 2C). Interestingly, there is a substantial broadening of the aromatic signals for Products A and B but not for DCPL. This is likely due to a chemical exchange process involving the ring systems, as the acetyl methyl signals of the lysine side chains are unaffected, but it is not related to oxidation, as the addition of the antioxidant ascorbate to the reaction halted the decay of each product but did not sharpen the aromatic signals (data not shown).

Product A is an Isoindole Derivative of DCPL. We next sought to characterize the products of DCPL autoxidation by purifying them from large scale reactions. Samples of purified Product A were dissolved in methanol and analyzed by LC-MS and 1D ^{1}H NMR (Figure 3). In the aliphatic region of its 1D ^{1}H NMR spectrum, Product A, like DCPL, contains a set of signals corresponding to a lysine side chain modified at the side chain N^{ζ} amine (Figure 3C). In the aromatic region, DCPL contains four signals: one singlet from its pyrrole ring and three from its catechol rings with their signature *J*-coupling pattern.

DOI: 10.1021/acs.biochem.7b01164
Biochemistry 2018, 57, 1462–1474

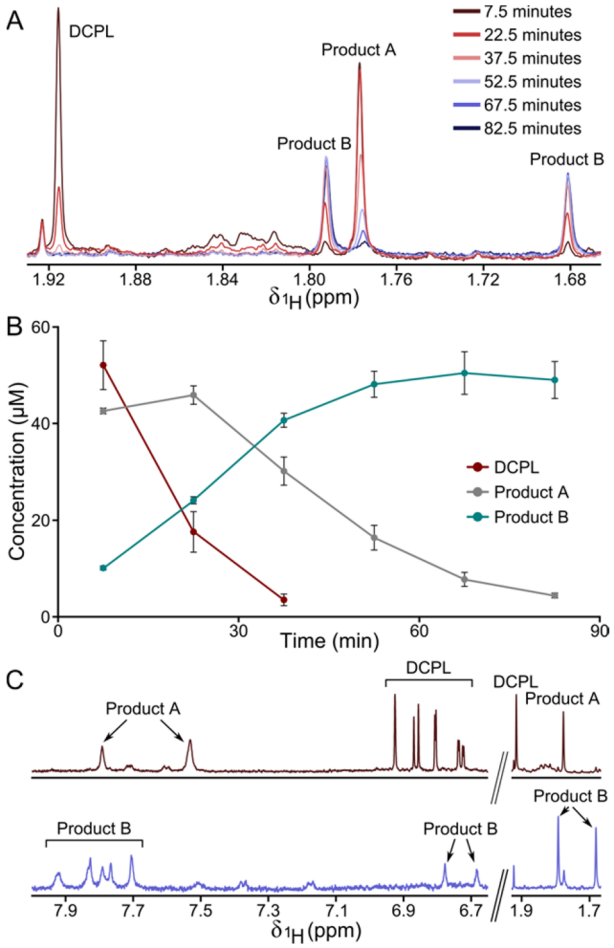

Figure 2. Dicatechol pyrrole lysine autoxidizes through an unstable intermediate species. (A) The autoxidation of 100 μM DCPL was tracked in PBS at 37 °C over the course of a 90 min incubation by monitoring its acetyl methyl signal in 1D ^{1}H NMR spectra. The DCPL signal decays rapidly, first producing a signal labeled Product A. Product A is unstable as well and is converted into two signals, together denoted Product B, that appear with similar kinetics and at nearly equivalent amounts. (B) The concentrations of the compounds in (A) were quantified using integrated signal intensities. Error bars represent standard deviations from three replicates. Product B represents the summation of the concentrations for the two similar secondary products. As Product B is later discovered to contain two methyl groups per molecule (Figure 4A), its concentration in this graph should be interpreted as twice the concentration of di-DCIL. (C) The aromatic regions of the 1D ^{1}H NMR spectra for incubation times of 7.5 (red) and 67.5 (blue) minutes are shown alongside their acetyl methyl regions. Note that whereas the aromatic signals for DCPL have narrow line widths, the aromatic signals of Products A and B are severely broadened.

Those four signals correspond to eight protons, as the symmetry of the DCPL ring system creates 2-fold chemical equivalency at each position. For Product A, there are only three aromatic signals, all singlets, with chemical shifts that are 0.5−1.0 ppm downfield of those of DCPLs. The symmetry of the Product A ring system is retained, as integrated intensities for each aromatic singlet match that of the lysine epsilon signal (which represents two protons). Thus, the conversion of DCPL to Product A requires a loss of two protons, at symmetric ring positions, leaving a set of ring protons that are not *J*-coupled to one another. These requirements are satisfied by the structure in Figure 3A, the product of an intramolecular reaction between

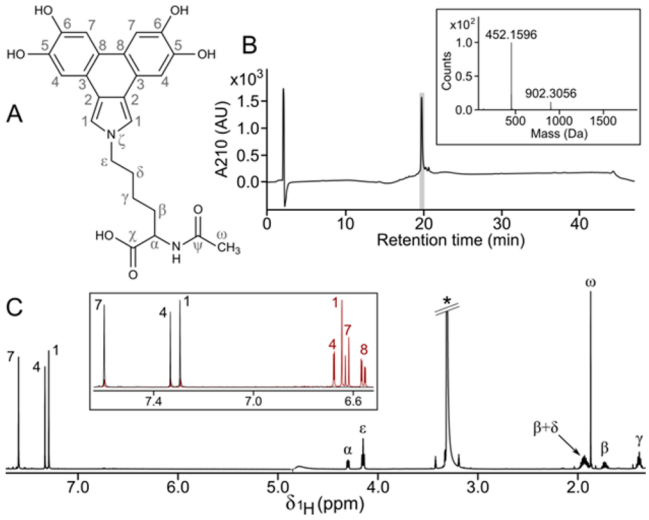

Figure 3. Characterization of reactive intermediate dicatechol isoindole lysine. (A) Annotated structure of DCIL. (B) LC-MS of purified DCIL. The inset shows the deconvoluted mass spectrum extracted from the shaded region of the LC profile. (C) 1D ^{1}H NMR spectrum of purified DCIL. An asterisk marks the methanol solvent peak. The inset is an overlay of the aromatic regions for DCIL (black) and DCPL (red). Formation of the DCIL isoindole group eliminates two DCPL ring protons, which due to their symmetry appear as a single signal in the DCPL spectrum (labeled 8) along with the loss of observable *J*-couplings and a large downfield shift for all three remaining ring protons of DCIL.

the catechol rings of DCPL to generate a new carbon−carbon bond and a fourth ring, and resulting in an isoindole moiety atop the lysine side chain nitrogen. The dicatechol isoindole lysine (DCIL) adduct has a calculated mass of 452.1584 Da in good agreement with the experimentally observed value of 452.1596 Da (Figure 3B). Its ring architecture was confirmed with 2D ^{1}H−^{13}C NMR spectra (Figure S1), and full ^{1}H and ^{13}C chemical shifts are listed in Table S1.

Product B is a Dimer of Two Dicatechol Isoindole Lysines. Product B was also purified from large scale DCPL autoxidation reactions, and samples were dissolved and characterized in methanol. We had initially interpreted the two acetyl methyl signals of Product B as arising from a single product; however, Product B eluted chromatographically as two separate species formed in essentially equivalent amounts. The products share very similar reverse-phase LC retention times (Figure 4B), experimentally indistinguishable masses (Figure 4C), and analogous 1D ^{1}H NMR spectra (Figure 4D). The large masses of the products clearly identify them as dimeric. Analysis of 2D ^{1}H−^{13}C spectra for the products revealed a common chemical structure, shown in Figure 4A, containing two DCILs joined by a carbon-carbon bond between the isoindole rings. We call this product didicatechol isoindole lysine (di-DCIL), and its calculated mass of 902.301 Da agrees well with the observed values (Figure 4B). Annotated 2D ^{1}H−^{13}C spectra for di-DCIL are shown in Figure S2, and full ^{1}H and ^{13}C chemical shifts are listed in Table S2. The di-DCIL compounds are fluorescent, and their excitation and emission spectra are reported in Figure S3.

The 1D ^{1}H NMR spectra of the two di-DCIL products illustrate their salient features (Figure 4D). For both products, the symmetry of each DCIL subunit's ring system is broken by the formation of the intermolecular linkage, giving rise to five

DOI: 10.1021/acs.biochem.7b01164
Biochemistry 2018, 57, 1462−1474

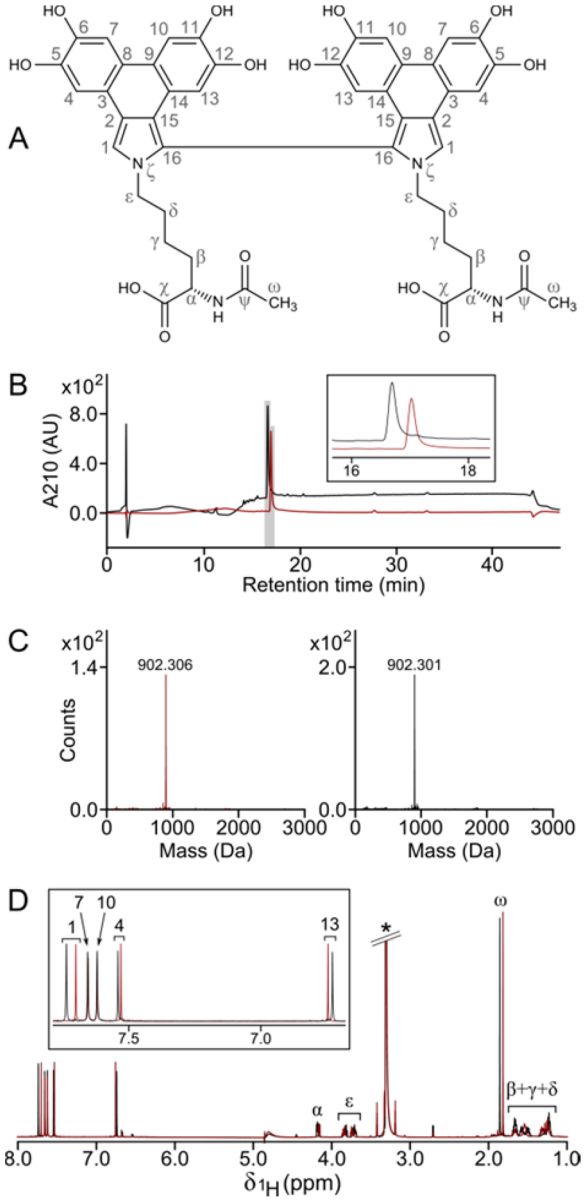

Figure 4. Characterization of dimeric didicatechol isoindole lysine. (A) Annotated structure of di-DCIL. (B–D) di-DCPL exists in two separable forms. In (B), chromatographic traces from LC-MS runs are shown for purified di-DCPL-1 (red) and di-DCPL-2 (black). The inset is a close-up view of the chromatographic peaks to illustrate the distinct retention times of the two dimeric species. In (C), deconvoluted mass spectra were extracted for di-DCPL-1 (red) and di-DCPL-2 (black) from the LC regions denoted by shaded squares in (B). An overlay of 1D ^{1}H NMR spectra for di-DCPL-1 (red) and di-DCPL-2 (black) is presented in (D) with an inset showing an expanded view of the aromatic region and labeling corresponding to the annotation in (A). In each di-DCPL species, symmetry across the intermolecular isoindole bond makes the two monomeric halves of the molecule chemically equivalent, thus giving a single set of NMR peaks. Observable deviations in chemical shifts between the two compounds occur in the aromatic rings (e.g., positions 1 and 13) and the acetyl methyl group (ω), whereas other signals are degenerate (e.g., 7 and 10).

singlets in the aromatic region representing the subunit's five ring protons. However, the dimer does contain symmetry across the new intermolecular bond, which imparts a new 2-fold chemical equivalency, such that the NMR signals for the two monomeric halves of the molecule are completely degenerate. This symmetry extends through the lysine side chain, and the aliphatic region of each spectrum contains a single set of resonances representing two identically modified lysines. The spectra for the two di-DCIL products are very similar, consistent with their shared chemical structure, but small differences in chemical shifts can be observed for the signals of the ring protons at the 1, 4, and 13 positions. The acetyl methyl signals (labeled ω) are also nondegenerate, which explains the two signals observed for Product B in the live monitoring of DCPL autoxidation by NMR (Figure 2A).

To verify that DCIL and di-DCIL are the two products observed during DCPL autoxidation and to confirm that they are intermediates in the predominant pathway of its decomposition, we collected 1D ^{1}H NMR spectra for unpurified samples withdrawn from the DCPL autoxidation reaction. Purified DCPL was incubated under the conditions described above, and aliquots were taken after 7.5 and 67.5 min, flash frozen in liquid nitrogen, lyophilized, and then resuspended into an equal volume of methanol, which prevents further oxidation of catechol-bearing compounds. In the 1D ^{1}H NMR spectra of the time points (Figure S4), the only observable aromatic signals belong to DCPL, DCIL, and di-DCIL in the amounts expected from the time course data in Figure 2A.

The Two di-DCIL Products Are Atropisomers. The identification of two di-DCILs, with common chemical structures but distinct chromatographic behavior and chemical shifts, prompted us to explore their chirality. In circular dichroism spectra, the two di-DCILs have similar absorbance profiles but opposite discriminations of polarity (Figure 5A), thus identifying them as complementary optically active isomers. The di-DCPL structure contains two chiral centers, at the α positions of the two lysines, and both must be in the S configuration, as the DCPL precursor is generated from reactions using pure L-form N_α-acetylated lysine. Racemization at the α positions could generate nonequivalent chiral centers and thus stereoisomers; however, conversion of D- and L-form amino acids is far too slow to be a factor in this reaction.[42] An alternative explanation is that restricted rotation around the intermolecular carbon-carbon bond between the DCIL subunits produces stable atropisomers. To estimate the energetic barrier to rotation about the intermolecular dihedral, defined by the two nitrogens of the di-DCIL and the carbons of the intermolecular bond, we calculated steric energies of energy-minimized models across all possible intermolecular dihedral angles. This analysis gave large energetic barriers of 110 and 30 kcal/mol for rotations passing through 0° (cis orientation of the ring systems) and 180° (trans orientation), respectively. Importantly, atropisomerism fully explains the structural nonequivalence of the two di-DCIL products. This point can be simply demonstrated by comparing the 3D structures of a di-DCIL enantiomer, which would have chemical shifts identical to its mirror image, and a di-DCIL atropisomer (Figure S5A–C). Although the enantiomer and atropisomer structures are similar, they are not superimposable, owing to their inverted chiralities at the lysine α positions. This structural difference generates nonequivalence in the conformational space sampled by the lysine backbone carboxylates of the two atropisomers, which may impact electrostatic interactions between the lysine backbone and the ring system and account for the nondegenerate aromatic chemical shifts of the two di-DCIL products.

DOI: 10.1021/acs.biochem.7b01164
Biochemistry 2018, 57, 1462–1474

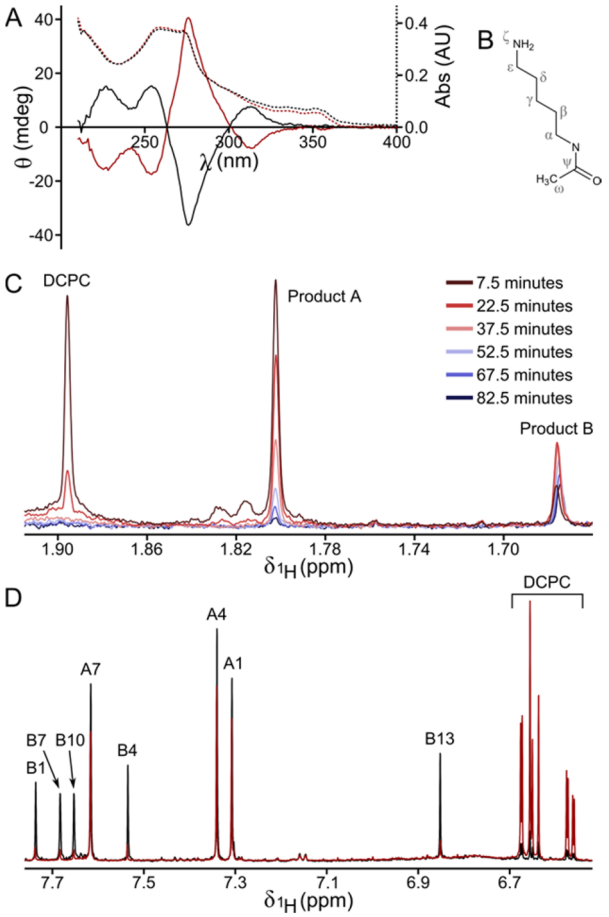

Figure 5. Lysine C_α chirality creates two stable, nonequivalent didicatechol isoindole lysine atropisomers. (A) CD spectra (solid lines) and UV−vis spectra (dashed lines) are shown for di-DCIL-1 (red) and di-DCIL-2 (black). The CD spectra exhibit the inverted profiles diagnostic of complementary optically active isomers. (B) Structure of N_α-acetylated cadaverine. The absence of a carboxylate group at the α position makes the compound achiral. (C) Autoxidation of 100 μM dicatechol pyrrole cadaverine at 37 °C in PBS was followed in 1D ^{1}H NMR spectra via its acetyl methyl signal. As with DCPL autoxidation, DCPC is first converted into an intermediate Product A, which then reacts further to yield Product B. Unlike DCPL autoxidation, Product B here has a single acetyl methyl signal. (D) 1D ^{1}H NMR spectra of stable time point samples taken after 7.5 (red) and 37.5 (black) minutes of DCPC autoxidation reveal the products' ring structures. Product A is the isoindole derivative of DCPC, analogous to DCIL. Product B is the isoindole-linked dimer; however, only one set of signals is observed, consistent with the chemical shift degeneracy of structurally equivalent atropisomers.

To confirm experimentally the role of chirality in producing nonequivalent atropisomers, we replaced the N_α-acetylated lysine component of DCPL with N_α-acetylated cadaverine (Figure 5B), which lacks a carboxylate at the α position and is therefore achiral. As shown in Figure S5D−F, this modification to di-DCIL yields a compound with an atropisomer that is structurally identical to its enantiomer. Therefore, although stable atropisomers exist, they should have completely degenerate chemical shifts.

Reactions between DOPAL and N_α-acetylated cadaverine produced dicatechol pyrrole cadaverine (DCPC) at a rate and amount analogous to those of DCPL (Figure S6A, B). DCPC was purified from large scale reactions, and its ^{1}H and ^{13}C chemical shifts are listed in Table S3. A comparison of 1D ^{1}H NMR spectra for DCPL and DCPC reveals a common set of aromatic signals with small differences in the ring proton chemical shifts that provide further evidence for electrostatic interactions between the rings and side chain base (Figure S6C). We next monitored the autoxidation of DCPC by 1D ^{1}H NMR in reactions analogous to those described for DCPL. As before, analysis of the acetyl methyl signals shows that autoxidation proceeds through a reactive intermediate, Product A (Figure 5C). In contrast to DCPL autoxidation, the decay of Product A in these reactions coincides with the appearance of only one Product B acetyl methyl signal (Figure 5C). By freezing time points from the autoxidation in liquid nitrogen, lyophilizing, and resuspending them in methanol, we were able to inhibit further oxidation and study the aromatic signals of the unpurified products by 1D ^{1}H NMR (Figure 5D). These spectra verify that Product A is the monomeric isoindole derivative of DCPC, analogous to DCIL. Although Product B has the five singlets belonging a dimer cross-linked through its isoindole rings, it has only a single set of aromatic signals, in contrast to di-DCIL but as expected for structurally equivalent atropisomers.

DOPAL-Based α-Synuclein Cross-Linking Occurs in Two Steps. We next explored whether the isoindole-based cross-linking pathway elucidated above establishes a relevant pathway for DOPAL-based oligomerization of α-synuclein in vitro. Under the standard reaction conditions of our prior study, with 100 μM N_α-acetylated α-synuclein (Ac-αS) and 2 mM DOPAL incubated at 37 °C at physiological pH, DCPL is produced nearly linearly at first with ~35% of the protein modified at the end of the first hour.[37] α-Synuclein contains 15 lysines for a total lysine concentration of 1.5 mM in our reactions, and DCPL is formed at a heterogeneous population of sites along its primary sequence. As in our prior study, the recombinant Ac-αS used here was bacterially expressed from a codon-optimized construct to preclude cysteine incorporation that results from mistranslation of residue Y136.[39] Native α-synuclein does not contain any cysteine residues.

Covalent cross-linking of proteins by small molecules requires two steps: (1) initial adduct formation between protein and small molecule and (2) further reaction of the adduct to form a linkage with a second protein. Our prior study identified DCPL as the predominant adduct formed within the first hour of reaction, at which point there is very little cross-linking, thereby leaving open the question of whether it is a relevant intermediate on a chemical pathway to cross-link formation. To answer this question, we used Cu(II) as a catalyst for α-synuclein cross-linking. Jinsmaa et al. first showed that Cu(II) dramatically stimulates DOPAL-based α-synuclein cross-linking,[33] and we were able to replicate that result using higher concentrations of reactants to visualize the protein oligomers by SDS-PAGE (Figure S7). In a reaction in 100 mM MOPS pH 7.4 with 100 μM Ac-αS, 2 mM DOPAL, and 100 μM DTPA to chelate any adventitious metals, very little protein cross-linking occurs over the course of a 60 min incubation at 37 °C. In contrast, when 500 μM $CuCl_2$ was added to the reaction (and the DTPA left out), we observed robust formation of oligomeric forms (dimer, trimer, tetramer, etc.) of the protein (Figure S7).

To test the cross-linking potential of initial DOPAL adducts, we performed a two-part reaction. In the first step, 100 μM Ac-αS was reacted with 2 mM DOPAL in 100 mM MOPS pH 7.4 with 100 μM DTPA at 37 °C with aliquots withdrawn every 20

DOI: 10.1021/acs.biochem.7b01164
Biochemistry 2018, 57, 1462−1474

min over the course of an hour incubation. The reacted protein was purified from excess DOPAL by ethanol precipitation, and the samples were then resuspended in the same volume of buffer without DTPA. In the second step, 500 μM $CuCl_2$ was added to each sample, and the samples were incubated at 37 °C with time points subjected to SDS-PAGE as shown in Figure 6A. Although the resuspended samples initially contained very

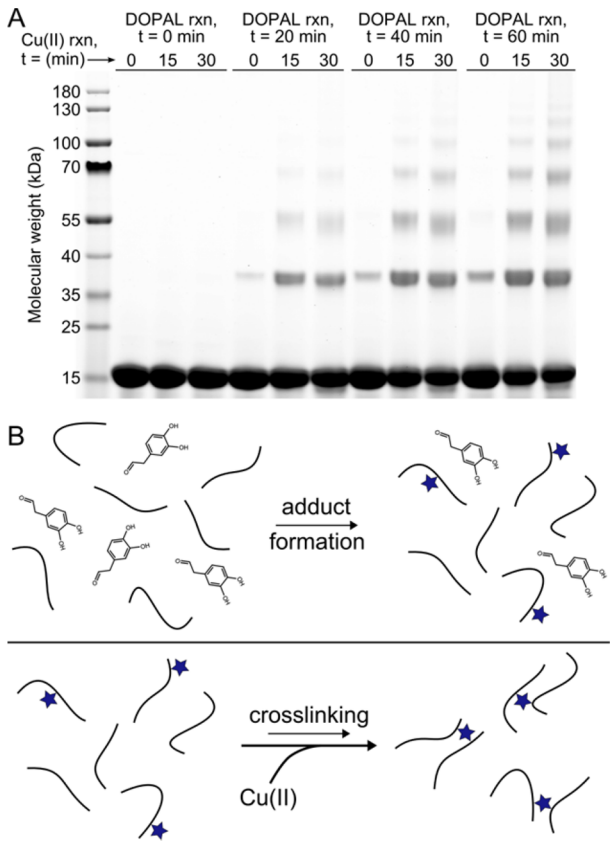

Figure 6. Adduct formation and cross-linking are separable steps in DOPAL-based oligomerization of α-synuclein. (A) Oligomer formation was monitored by SDS-PAGE for the two-part reaction. In the first step, α-synuclein was incubated with DOPAL for an hour with aliquots taken at the indicated times, and the samples were purified by ethanol precipitation to remove excess DOPAL. In the second step, addition of Cu(II) induced rapid formation of covalent oligomers with the cross-links nearly completely formed within the first 15 min. The amount of oligomers produced in the cross-linking step is dependent on the length of the first incubation with DOPAL. Initial time points (t = 0) were taken immediately prior to the addition of DOPAL or Cu(II). (B) Schematic of DOPAL-based cross-linking of α-synuclein. In the first step, DOPAL reacts with α-synuclein to form DCPL adducts (blue stars). In the second step, the adducts react further to form oligomers. The cross-linking step can be accelerated by Cu(II) and other catechol oxidants.

small amounts of protein oligomers, the addition of Cu(II) led to rapid formation of interprotein cross-links with the reaction near completion by the first 15 min time point. Importantly, the amount of cross-linked protein increased with the length of the DOPAL incubation in the first step, indicating that an increase in adduct formation during the first DOPAL incubation led directly to an increased capacity for cross-linking. Cu(II) had no effect on unreacted protein (DOPAL rxn, t = 0 lanes in Figure 6A).

DCPL has two catechol rings, and Cu(II) is known to oxidize catechols.[43] To verify that Cu(II) played the role of an oxidant in our two-part reaction, we performed reactions analogous to those in Figure 6A but with 500 μM sodium periodate ($NaIO_4$), which is also known to oxidize catechols efficaciously,[44] in place of $CuCl_2$. This again led to the rapid formation of oligomers with the reaction again nearly complete within the first 15 min (Figure S8). Catechols also autoxidize in a chain reaction initiated by molecular oxygen and propagated by the superoxide radical.[8,9] To confirm that autoxidation of the DOPAL adducts also leads to cross-linking, we performed a third reaction in which the samples in the second step were incubated at 37 °C without an oxidant. We again observed oligomer formation, although in this case the cross-links formed more slowly with 2−3 h required for maximal production of oligomers (Figure S8).

Our results elucidate a two-step reaction for DOPAL-based cross-linking of α-synuclein, illustrated in Figure 6B. In the first step, DOPAL reacts with α-synuclein's lysines with robust modification of the protein during an hour-long incubation at 37 °C despite the absence of interprotein cross-links. In the second step, the covalent DOPAL adducts react further to produce intermolecular protein cross-links. Although the second step occurs by autoxidation, it can be significantly accelerated by the addition of oxidants.

DOPAL Adducts Preferentially Form Cross-Links with Other Adducts. Next, we exploited the two-step nature of the cross-linking reaction to explore its mechanism. We considered two potential pathways for cross-link formation. In the first, the DOPAL adduct on one protein reacts with a native moiety (e.g., an unmodified lysine side chain) of a second protein, forming an adduct-to-protein cross-link as proposed by others.[35] In the alternative pathway, the DOPAL adduct reacts with a DOPAL adduct on a second protein, forming an adduct-to-adduct cross-link. To discriminate between cross-linking pathways, we devised an experiment utilizing different isotopically labeled Ac-αS samples illustrated by the schematic in Figure 7A. First, nonisotopically labeled Ac-αS was reacted with DOPAL to form adducts under conditions that discourage cross-linking (20 μM protein, 2 mM DOPAL, 30 min incubation at 37 °C in PBS with 100 μM DTPA) and then purified from excess DOPAL by ethanol precipitation. The DOPAL-reacted, nonisotopically labeled protein was resuspended at 100 μM concentration with an equal amount of unreacted, $^1H/^{15}N$-labeled Ac-αS in PBS with 100 μM DTPA and incubated at 37 °C for 4 h to allow cross-links to form. In the event that cross-linking occurs entirely by the adduct-to-protein pathway, the DOPAL-reacted protein will form cross-links equally well with native reactive groups on nonisotopically labeled and $^1H/^{15}N$-labeled proteins, leading to oligomers containing 25% $^1H/^{15}N$-labeled Ac-αS. On the other hand, if cross-linking proceeds only by the adduct-to-adduct mechanism, the resulting oligomers will be entirely composed of nonisotopically labeled protein, as the $^1H/^{15}N$-labeled protein is unreacted and does not have DOPAL adducts.

We were able to purify the oligomeric fraction of the isotopically mixed cross-linking reaction by size exclusion chromatography (Figure 7B), and its isotopic composition was assessed by ^1H NMR. The simple pulse sequence described and benchmarked in Figure S9 uses phase cycling to either select or filter ^{15}N-coupled protons, giving two 1D ^1H NMR spectra that quantitatively report the fraction of $^1H/^{15}N$-labeled protein in a sample. As the maximum expected incorporation of $^1H/^{15}N$-

DOI: 10.1021/acs.biochem.7b01164
Biochemistry 2018, 57, 1462−1474

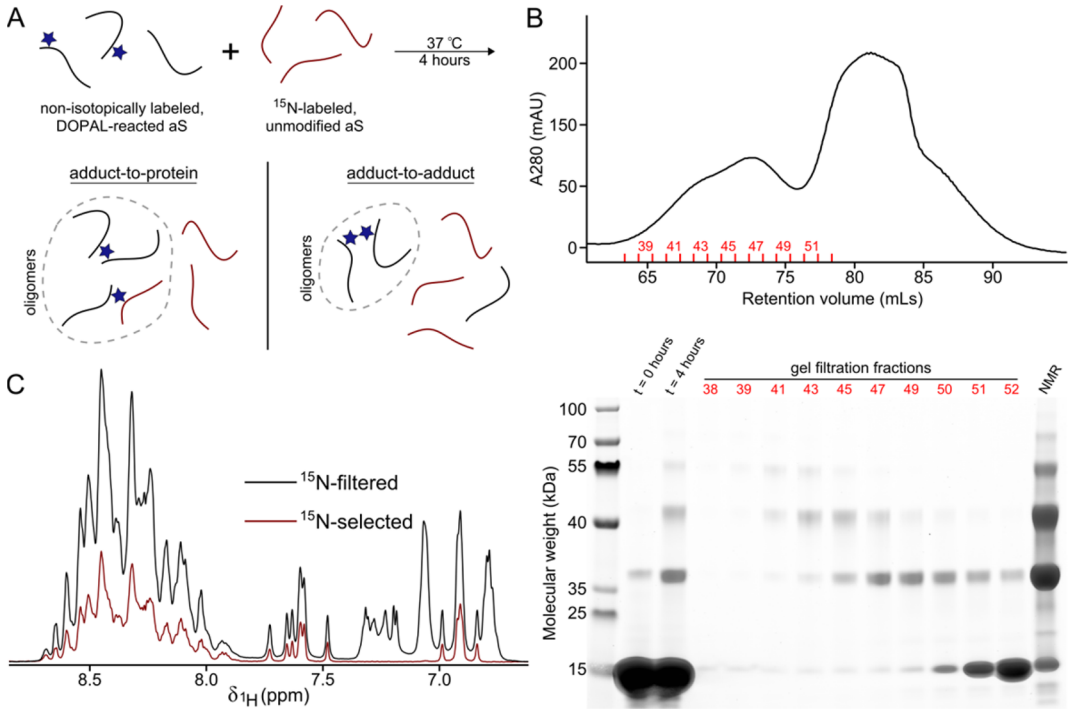

Figure 7. DOPAL cross-linking mechanism probed with an isotopic labeling-based approach. (A) Schematic illustrating the experimental strategy and the two potential cross-linking mechanisms. Nonisotopically labeled α-synuclein (black) was reacted with DOPAL to form adducts (blue stars) and then purified from the excess DOPAL by ethanol precipitation, and an equimolar amount of unmodified ^{15}N-labeled α-synuclein (red) was added. Cross-links were formed by incubating the sample at 37 °C for 4 h. Cross-links may form by reaction of the adducts with native protein side chains, in which case the oligomers will contain a 3:1 ratio of nonisotopically labeled to ^{15}N-labeled α-synuclein. Alternatively, cross-links may form by reaction between adducts, producing oligomers that are entirely composed of nonisotopically labeled protein. (B) Purification of DOPAL-induced oligomers. Oligomers in the mixed nonisotopically and ^{15}N-labeled α-synuclein were purified from the monomers by gel filtration. The top panel shows the chromatographic trace with oligomer-containing fractions labeled. In the bottom panel, the fractions were analyzed by SDS-PAGE along with the final oligomer NMR sample, which was prepared by combining and concentrating fractions 39−50, and samples taken before and after the cross-linking incubation period. (C) The cross-linking mechanism was assessed by measuring the incorporation of ^{15}N-labeled α-synuclein into the purified DOPAL oligomers with ^{15}N-filtered and -selected 1D ^{1}H amide proton spectra. The ^{15}N-selected spectrum was collected with three times the number of scans of the ^{15}N-filtered spectrum, so that cross-linking through the adduct-to-protein mechanism in (A) would give spectra of equal intensity. Instead, the integrated intensity of the ^{15}N-selected amide protons is 34% that of ^{15}N-filtered ones, indicating that adduct-to-adduct cross-linking is the predominant mechanism of oligomer formation.

labeled protein into the oligomers is 25%, the ^{15}N-selected ^{1}H spectrum was collected with three times as many scans as the ^{15}N-filtered spectrum. For cross-linking entirely through an adduct-to-protein mechanism, producing oligomers containing 25% ^{1}H/^{15}N-labeled protein and 75% nonisotopically labeled protein (a 1:3 molar ratio), the two spectra will have equal intensity (Figure S9D). When we collected the spectra for the purified oligomers, we instead observed that the ^{15}N-filtered spectrum had much greater intensity than the ^{15}N-labeled one (Figure 7C). By integrating the amide regions of each spectrum, with a small correction to account for incomplete suppression of ^{1}H/^{15}N-labeled signals by the ^{15}N-filter (Figure S9C), we calculate that the cross-linked oligomers contain 8.6% ^{1}H/^{15}N-labeled protein, indicating that although both cross-linking mechanisms occur, the adduct-to-adduct pathway predominates. This value also likely represents a conservative estimate of the preference for adduct-to-adduct cross-linking, as the oligomeric fraction could not be perfectly separated from monomer, which is composed of >50% ^{1}H/^{15}N-labeled protein and thus would artificially inflate the measured incorporation of ^{1}H/^{15}N-labeled protein into the oligomers.

The incorporation of ^{1}H/^{15}N-labeled Ac-αS into the oligomers offered the opportunity to probe the sites of adduct-to-protein cross-linking by NMR. In a ^{1}H/^{15}N HSQC spectrum of the oligomer sample, loss of native intensity for the amide groups will occur for residues at or near the cross-links that tether the otherwise unmodified protein into the oligomers. Additional loss will result from changes in transient electrostatic interactions from both disrupted intramolecular contacts and newly introduced intermolecular ones that heterogeneously broaden the amide signals. The pattern of normalized signal loss observed for the oligomer sample across the α-synuclein primary sequence is complex (Figure S10) with a large and broad decrease for the N-terminal 60 residues. A similar pattern was observed for modification of α-synuclein by DOPAL,[34,35,37] which produces a heterogeneous population of DCPL adducts on the 15 lysine residues that are concentrated in the N-terminal half of the protein. However, the pattern observed here also features a significant loss of intensity at the C-terminus, which does not contain lysine. Comparison of peaks in the oligomer sample and an unmodified control reveals multiple causes for the loss of native peak intensity (Figure S11). We did not observe new signals corresponding to the methionine-oxidized form of α-synuclein that would attribute native signal loss to sulfoxide formation.

Mass Spectrum of DOPAL Cross-Linked α-Synuclein Dimer. To further investigate whether di-DCIL cross-links play a role in DOPAL-induced oligomerization of α-synuclein, we

DOI: 10.1021/acs.biochem.7b01164
Biochemistry 2018, 57, 1462−1474

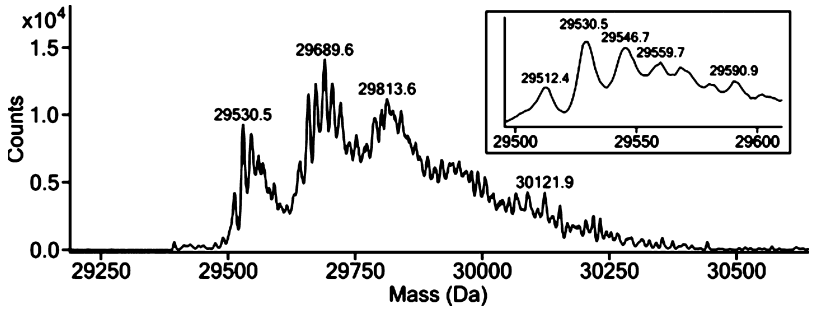

Figure 8. Deconvoluted mass spectrum of a purified dimeric fraction of DOPAL cross-linked α-synuclein. The mass peak at 29530.50 Da is consistent with an α-synuclein dimer linked by di-DCIL. The spectrum contains a significant amount of heterogeneity with many overlapping mass peaks, nearly all of which have higher molecular weights than the di-DCIL-linked dimer. The inset shows an expanded view of the first cluster of peaks containing the di-DCIL-linked dimer. No peaks were observed outside of the mass range shown here except for a small, heterogeneous group in the monomeric α-synuclein mass range with a total area less than 5% of those in the dimeric region.

purified a sample of dimeric protein from a DOPAL cross-linking reaction and studied it by mass spectrometry. To prepare the sample, we used a similar two-step strategy as in our isotopic labeling experiment. The initial adduct forming step was performed under conditions that suppress cross-links with 20 μM nonisotopically labeled Ac-αS and 2 mM DOPAL incubated for 30 min at 37 °C in PBS with 100 μM DTPA. After removal of excess DOPAL by ethanol precipitation, the reacted protein was resuspended at 100 μM concentration in PBS with 100 μM DTPA and then incubated at 37 °C to generate cross-links. After 4 h, ascorbate was added to a concentration of 10 mM to terminate the reaction and prevent oxidative degradation of the cross-links. Dimeric protein was purified from monomers and higher order oligomers by size exclusion chromatography, which was run with 10 mM ascorbate in the buffer. Purified α-synuclein dimer was buffer exchanged into water and directly injected into the mass spectrometer without chromatographic separation, giving the mass spectrum shown in Figure 8. The observed spectrum is complex with several sets of overlapping peaks spanning a range of ∼600 Da. The predominant peak in the cluster at the lower end of the observed masses corresponds to a dimer of 29530.5 Da, which is within the experimental error for an α-synuclein dimer cross-linked by a di-DCIL linkage (expected mass of 29530.9 Da). Notably, the only substantial peak with a smaller mass (29512.4 Da, inset of Figure 8) likely represents a loss of water (18 Da) from the di-DCIL-linked dimer species, an artifact that is commonly observed in protein mass spectra. The peak with a mass just larger than the di-DCIL-linked protein is +16 Da and likely results from oxidation of one of the eight methionine residues in the dimer. DOPAL is known to cause oxidation of α-synuclein's methionines,[35] and in the dimer sample preparation, this must occur predominantly in the adduct forming step as no oxidized methionine was observed by NMR in the isotopic labeling experiment (Figure 7) for the $^{1}H/^{15}N$-labeled portion of the oligomers that was present only during the cross-linking step of the reaction. The remainder of the heterogeneous peaks correspond to unknown dimeric species with masses larger than the expected di-DCIL-linked product.

DISCUSSION

In this study, we build on our previous work identifying DCPL as the predominant adduct formed in reactions between DOPAL and α-synuclein by describing a pathway for DCPL-based cross-linking. Like DOPAL reactivity, cross-linking is driven by catechol oxidation, providing another connection between the catecholaldehyde hypothesis, α-synuclein oligomerization, and redox imbalance, which is a well-established contributor to PD etiology. A key intermediate in the cross-linking pathway is DCIL formed by an intramolecular reaction between the catechol rings of DCPL to generate a core isoindole structure. This preliminary step appears to be required to activate the reactivity of the adduct at the nitrogen-adjacent ring position, as we were unable to observe dimeric products containing DCPL. The instability of DCIL is not unexpected as the isoindole group is known to be highly reactive and prone to autoxidation.[45] In fact, the parent isoindole compound resisted isolation and characterization until the 1970s, over 100 years after its structural isomer indole. Isoindole autoxidation yields polymers, although the chemistry of these reactions is poorly understood owing in part to the heterogeneity of products and the strong influence of reaction conditions and ring substituents. A general principle, however, is that isoindole reactions occur at the nitrogen-adjacent carbons, and dimeric products formed by cross-linking at those positions, like di-DCIL, have been reported.[45]

Several observations support the relevance of a DCPL-based in vitro cross-linking mechanism for α-synuclein. DCPL adducts form early in the reaction between DOPAL and α-synuclein;[37] these early products are capable of forming cross-links (Figure 6 and Figure S7), and the results from our isotopic labeling-based test with α-synuclein (Figure 7) indicate that cross-linking primarily occurs through an adduct-to-adduct mechanism. We were also able to directly observe the di-DCIL-linked species in the mass spectrum of a purified dimeric α-synuclein sample (Figure 8). The spectrum for this sample also contains a considerable number of other mass peaks with molecular weights up to ∼600 Da larger than the di-DCIL dimer. The cause of the observed heterogeneity is unknown. Notably, we were unable to observe a mass peak that would represent dimeric α-synuclein with a cross-link composed of a single DOPAL molecule, as expected for the alternative mechanism for DOPAL-based cross-linking proposed by others and discussed in more detail below.

Other groups have studied DOPAL reactivity. Both Schiff base and Michael addition products, resulting from reaction of the lysine side chain amine with the aldehyde and catechol ring, respectively, of a single DOPAL, were observed in DOPAL-reacted α-synuclein samples.[34,35] Interpretation of these results is hampered by their lack of quantification, as well as the lengthy incubations and/or harsh conditions required for

DOI: 10.1021/acs.biochem.7b01164
Biochemistry 2018, 57, 1462−1474

proteolytic digestion of LC-MS samples that may preclude the identification of unstable adducts like DCPL. In a reaction with DOPAL and a lysine-containing model peptide studied by MS, Rees et al. observed a Schiff base but no Michael addition product.[7] Although the Schiff base was attributed to the peptide's lysine residue, the peptide also contained an unprotected N-terminal amine, which can readily form Schiff base products;[37] an unidentified product with a mass corresponding to a DCPL adduct was also observed.[7] Outside of our work here, no DOPAL-based cross-linked product has been isolated and characterized.

An alternative cross-linking mechanism proposes that cross-links consist of a single DOPAL, covalently connecting two lysines through linkages at its aldehyde and catechol moiety.[35] Two lines of reasoning argue against this mechanism. First, DOPAL potently catalyzes α-synuclein oligomer formation in vitro. Being intrinsically disordered, the concentration of potential intramolecular lysine targets presented to an α-synuclein DOPAL adduct far exceeds the concentration of intermolecular ones. Thus, cross-linking by the alternative mechanism would primarily yield intramolecular linkages and very few intermolecular ones, as observed for the dilysine cross-linker disuccinimidyl glutarate in the absence of membranes.[46] The predominant adduct-to-adduct mechanism reported here, on the other hand, favors the experimentally observed formation of intermolecular cross-links. Second, Schiff bases cannot provide a stable chemical scaffold for covalent cross-linking as they are transient products of a reversible reaction. In an analogous fashion, protein cross-linking by advanced glycation end-products begins with the formation of transient Schiff base products between sugar aldehydes and lysine side chain amines.[47] An Amadori rearrangement then converts the Schiff base to a stable secondary amine, and this step is an essential prerequisite for forming cross-linked products.[47] The Amadori rearrangement requires a hydroxyl on the sugar carbon adjacent to the Schiff base, and therefore, an equivalent reaction is not possible with DOPAL.

Accumulating evidence suggests a link between PD and aberrant levels of the reactive dopamine metabolite DOPAL.[2] DOPAL may exert its toxicity by forming adducts with α-synuclein that disrupt its cellular function and localization, for example, by impairing its membrane binding[34,35] and by catalyzing covalent cross-links that nucleate toxic oligomeric species or stabilize them, possibly by terminating in-register fibril elongation. Despite the potential importance of the catecholaldehyde hypothesis in PD etiology, the products of DOPAL reactivity remain poorly characterized in comparison with protein modification by other small molecules. Although the in vitro experiments described here lack the complexity of cellular antioxidants, membrane binding surfaces, and other possible modulators of DOPAL reactivity, we expect that the underlying chemistry revealed by this study will prove useful in the development of assays that can identify DOPAL-based cross-links in vivo. Such tools will be imperative for a rigorous test of the catecholaldehyde hypothesis and determination of the role of DOPAL in PD neurodegeneration.

■ ASSOCIATED CONTENT

Supporting Information

The Supporting Information is available free of charge on the ACS Publications website at DOI: 10.1021/acs.biochem.7b01164.

NMR and optical spectra and chemical shift tables of dicatechol isoindole lysine and related products, NMR spectra of mixed isotopic labeling experiments to identify cross-linking, and SDS-PAGE gel figures monitoring cross-linking (PDF)

■ AUTHOR INFORMATION

Corresponding Authors

*E-mail: rlevine@nih.gov.
*E-mail: bax@nih.gov.

ORCID

Ad Bax: 0000-0002-9809-5700

Funding

This work was supported by the Intramural Research Programs of the National Institute of Diabetes and Digestive and Kidney Diseases (project ZIA DK029047) and the National Heart, Lung, and Blood Institute (project ZIA HL000225).

Notes

The authors declare no competing financial interest.

■ ACKNOWLEDGMENTS

We thank Daniel Mulvihill (University of Kent) for the NatB acetyltransferase construct, Carole Bewley (NIDDK) and Jinfa Ying (NIDDK) for insightful discussions and advice, and Joseph Courtney (NIDDK) for help with data analysis. Fluorescence measurements were performed in the Biophysics Core Facility of the National, Heart, Lung, and Blood Institute.

■ REFERENCES

(1) Blaschko, H. (1952) Amine oxidase and amine metabolism. *Pharmacol Rev. 4*, 415−458.

(2) Goldstein, D. S., Kopin, I. J., and Sharabi, Y. (2014) Catecholamine autotoxicity. Implications for pharmacology and therapeutics of Parkinson disease and related disorders. *Pharmacol. Ther. 144*, 268−282.

(3) Burke, W. J., Li, S. W., Chung, H. D., Ruggiero, D. A., Kristal, B. S., Johnson, E. M., Lampe, P., Kumar, V. B., Franko, M., Williams, E. A., and Zahm, D. S. (2004) Neurotoxicity of MAO metabolites of catecholamine neurotransmitters: role in neurodegenerative diseases. *NeuroToxicology 25*, 101−115.

(4) Goldstein, D. S., Sullivan, P., Cooney, A., Jinsmaa, Y., Sullivan, R., Gross, D. J., Holmes, C., Kopin, I. J., and Sharabi, Y. (2012) Vesicular uptake blockade generates the toxic dopamine metabolite 3,4-dihydroxyphenylacetaldehyde in PC12 cells: relevance to the pathogenesis of Parkinson's disease. *J. Neurochem. 123*, 932−943.

(5) Mattammal, M. B., Haring, J. H., Chung, H. D., Raghu, G., and Strong, R. (1995) An endogenous dopaminergic neurotoxin: implication for Parkinson's disease. *Neurodegeneration 4*, 271−281.

(6) Burke, W. J., Li, S. W., Williams, E. A., Nonneman, R., and Zahm, D. S. (2003) 3,4-Dihydroxyphenylacetaldehyde is the toxic dopamine metabolite in vivo: implications for Parkinson's disease pathogenesis. *Brain Res. 989*, 205−213.

(7) Rees, J. N., Florang, V. R., Eckert, L. L., and Doorn, J. A. (2009) Protein reactivity of 3,4-dihydroxyphenylacetaldehyde, a toxic dopamine metabolite, is dependent on both the aldehyde and the catechol. *Chem. Res. Toxicol. 22*, 1256−1263.

(8) Werner-Allen, J. W., Levine, R. L., and Bax, A. (2017) Superoxide is the critical driver of DOPAL autoxidation, lysyl adduct formation, and crosslinking of alpha-synuclein. *Biochem. Biophys. Res. Commun. 487*, 281−286.

(9) Misra, H. P., and Fridovich, I. (1972) The role of superoxide anion in the autoxidation of epinephrine and a simple assay for superoxide dismutase. *J. Biol. Chem. 247*, 3170−3175.

DOI: 10.1021/acs.biochem.7b01164
Biochemistry 2018, 57, 1462−1474

(10) Goldstein, D. S., Sullivan, P., Holmes, C., Kopin, I. J., Basile, M. J., and Mash, D. C. (2011) Catechols in post-mortem brain of patients with Parkinson disease. *Eur. J. Neurol 18*, 703−710.
(11) Liu, G., Yu, J., Ding, J., Xie, C., Sun, L., Rudenko, I., Zheng, W., Sastry, N., Luo, J., Rudow, G., Troncoso, J. C., and Cai, H. (2014) Aldehyde dehydrogenase 1 defines and protects a nigrostriatal dopaminergic neuron subpopulation. *J. Clin. Invest. 124*, 3032−3046.
(12) Grunblatt, E., Mandel, S., Jacob-Hirsch, J., Zeligson, S., Amariglo, N., Rechavi, G., Li, J., Ravid, R., Roggendorf, W., Riederer, P., and Youdim, M. B. (2004) Gene expression profiling of parkinsonian substantia nigra pars compacta; alterations in ubiquitin-proteasome, heat shock protein, iron and oxidative stress regulated proteins, cell adhesion/cellular matrix and vesicle trafficking genes. *J. Neural Transm (Vienna) 111*, 1543−1573.
(13) Wey, M. C., Fernandez, E., Martinez, P. A., Sullivan, P., Goldstein, D. S., and Strong, R. (2012) Neurodegeneration and motor dysfunction in mice lacking cytosolic and mitochondrial aldehyde dehydrogenases: implications for Parkinson's disease. *PLoS One 7*, e31522.
(14) Casida, J. E., Ford, B., Jinsmaa, Y., Sullivan, P., Cooney, A., and Goldstein, D. S. (2014) Benomyl, aldehyde dehydrogenase, DOPAL, and the catecholaldehyde hypothesis for the pathogenesis of Parkinson's disease. *Chem. Res. Toxicol. 27*, 1359−1361.
(15) Doorn, J. A., Florang, V. R., Schamp, J. H., and Vanle, B. C. (2014) Aldehyde dehydrogenase inhibition generates a reactive dopamine metabolite autotoxic to dopamine neurons. *Parkinsonism Relat Disord 20* (Suppl 1), S73−75.
(16) Fitzmaurice, A. G., Rhodes, S. L., Lulla, A., Murphy, N. P., Lam, H. A., O'Donnell, K. C., Barnhill, L., Casida, J. E., Cockburn, M., Sagasti, A., Stahl, M. C., Maidment, N. T., Ritz, B., and Bronstein, J. M. (2013) Aldehyde dehydrogenase inhibition as a pathogenic mechanism in Parkinson disease. *Proc. Natl. Acad. Sci. U. S. A. 110*, 636−641.
(17) Trinh, J., and Farrer, M. (2013) Advances in the genetics of Parkinson disease. *Nat. Rev. Neurol. 9*, 445−454.
(18) Dikiy, I., and Eliezer, D. (2012) Folding and misfolding of alpha-synuclein on membranes. *Biochim. Biophys. Acta, Biomembr. 1818*, 1013−1018.
(19) Auluck, P. K., Caraveo, G., and Lindquist, S. (2010) alpha-Synuclein: membrane interactions and toxicity in Parkinson's disease. *Annu. Rev. Cell Dev. Biol. 26*, 211−233.
(20) Burre, J., Sharma, M., Tsetsenis, T., Buchman, V., Etherton, M. R., and Sudhof, T. C. (2010) Alpha-synuclein promotes SNARE-complex assembly in vivo and in vitro. *Science 329*, 1663−1667.
(21) Maltsev, A. S., Chen, J., Levine, R. L., and Bax, A. (2013) Site-specific interaction between alpha-synuclein and membranes probed by NMR-observed methionine oxidation rates. *J. Am. Chem. Soc. 135*, 2943−2946.
(22) Schildknecht, S., Gerding, H. R., Karreman, C., Drescher, M., Lashuel, H. A., Outeiro, T. F., Di Monte, D. A., and Leist, M. (2013) Oxidative and nitrative alpha-synuclein modifications and proteostatic stress: implications for disease mechanisms and interventions in synucleinopathies. *J. Neurochem. 125*, 491−511.
(23) Binolfi, A., Limatola, A., Verzini, S., Kosten, J., Theillet, F. X., Rose, H. M., Bekei, B., Stuiver, M., van Rossum, M., and Selenko, P. (2016) Intracellular repair of oxidation-damaged alpha-synuclein fails to target C-terminal modification sites. *Nat. Commun. 7*, 10251.
(24) Lashuel, H. A., Overk, C. R., Oueslati, A., and Masliah, E. (2013) The many faces of alpha-synuclein: from structure and toxicity to therapeutic target. *Nat. Rev. Neurosci. 14*, 38−48.
(25) Tuttle, M. D., Comellas, G., Nieuwkoop, A. J., Covell, D. J., Berthold, D. A., Kloepper, K. D., Courtney, J. M., Kim, J. K., Barclay, A. M., Kendall, A., Wan, W., Stubbs, G., Schwieters, C. D., Lee, V. M., George, J. M., and Rienstra, C. M. (2016) Solid-state NMR structure of a pathogenic fibril of full-length human alpha-synuclein. *Nat. Struct. Mol. Biol. 23*, 409−415.
(26) Conway, K. A., Lee, S. J., Rochet, J. C., Ding, T. T., Harper, J. D., Williamson, R. E., and Lansbury, P. T., Jr. (2000) Accelerated oligomerization by Parkinson's disease linked alpha-synuclein mutants. *Ann. N. Y. Acad. Sci. 920*, 42−45.
(27) Conway, K. A., Lee, S. J., Rochet, J. C., Ding, T. T., Williamson, R. E., and Lansbury, P. T., Jr. (2000) Acceleration of oligomerization, not fibrillization, is a shared property of both alpha-synuclein mutations linked to early-onset Parkinson's disease: implications for pathogenesis and therapy. *Proc. Natl. Acad. Sci. U. S. A. 97*, 571−576.
(28) Winner, B., Jappelli, R., Maji, S. K., Desplats, P. A., Boyer, L., Aigner, S., Hetzer, C., Loher, T., Vilar, M., Campioni, S., Tzitzilonis, C., Soragni, A., Jessberger, S., Mira, H., Consiglio, A., Pham, E., Masliah, E., Gage, F. H., and Riek, R. (2011) In vivo demonstration that alpha-synuclein oligomers are toxic. *Proc. Natl. Acad. Sci. U. S. A. 108*, 4194−4199.
(29) Almandoz-Gil, L., Welander, H., Ihse, E., Khoonsari, P. E., Musunuri, S., Lendel, C., Sigvardson, J., Karlsson, M., Ingelsson, M., Kultima, K., and Bergstrom, J. (2017) Low molar excess of 4-oxo-2-nonenal and 4-hydroxy-2-nonenal promote oligomerization of alpha-synuclein through different pathways. *Free Radical Biol. Med. 110*, 421−431.
(30) Iljina, M., Tosatto, L., Choi, M. L., Sang, J. C., Ye, Y., Hughes, C. D., Bryant, C. E., Gandhi, S., and Klenerman, D. (2016) Arachidonic acid mediates the formation of abundant alpha-helical multimers of alpha-synuclein. *Sci. Rep. 6*, 33928.
(31) Vicente Miranda, H., Szego, E. M., Oliveira, L. M. A., Breda, C., Darendelioglu, E., de Oliveira, R. M., Ferreira, D. G., Gomes, M. A., Rott, R., Oliveira, M., Munari, F., Enguita, F. J., Simoes, T., Rodrigues, E. F., Heinrich, M., Martins, I. C., Zamolo, I., Riess, O., Cordeiro, C., Ponces-Freire, A., Lashuel, H. A., Santos, N. C., Lopes, L. V., Xiang, W., Jovin, T. M., Penque, D., Engelender, S., Zweckstetter, M., Klucken, J., Giorgini, F., Quintas, A., and Outeiro, T. F. (2017) Glycation potentiates alpha-synuclein-associated neurodegeneration in synucleinopathies. *Brain 140*, 1399−1419.
(32) Burke, W. J., Kumar, V. B., Pandey, N., Panneton, W. M., Gan, Q., Franko, M. W., O'Dell, M., Li, S. W., Pan, Y., Chung, H. D., and Galvin, J. E. (2008) Aggregation of alpha-synuclein by DOPAL, the monoamine oxidase metabolite of dopamine. *Acta Neuropathol. 115*, 193−203.
(33) Jinsmaa, Y., Sullivan, P., Gross, D., Cooney, A., Sharabi, Y., and Goldstein, D. S. (2014) Divalent metal ions enhance DOPAL-induced oligomerization of alpha-synuclein. *Neurosci. Lett. 569*, 27−32.
(34) Plotegher, N., Berti, G., Ferrari, E., Tessari, I., Zanetti, M., Lunelli, L., Greggio, E., Bisaglia, M., Veronesi, M., Girotto, S., Dalla Serra, M., Perego, C., Casella, L., and Bubacco, L. (2017) DOPAL derived alpha-synuclein oligomers impair synaptic vesicles physiological function. *Sci. Rep. 7*, 40699.
(35) Follmer, C., Coelho-Cerqueira, E., Yatabe-Franco, D. Y., Araujo, G. D., Pinheiro, A. S., Domont, G. B., and Eliezer, D. (2015) Oligomerization and Membrane-binding Properties of Covalent Adducts Formed by the Interaction of alpha-Synuclein with the Toxic Dopamine Metabolite 3,4-Dihydroxyphenylacetaldehyde (DOPAL). *J. Biol. Chem. 290*, 27660−27679.
(36) Anderson, D. G., Florang, V. R., Schamp, J. H., Buettner, G. R., and Doorn, J. A. (2016) Antioxidant-Mediated Modulation of Protein Reactivity for 3,4-Dihydroxyphenylacetaldehyde, a Toxic Dopamine Metabolite. *Chem. Res. Toxicol. 29*, 1098−1107.
(37) Werner-Allen, J. W., DuMond, J. F., Levine, R. L., and Bax, A. (2016) Toxic Dopamine Metabolite DOPAL Forms an Unexpected Dicatechol Pyrrole Adduct with Lysines of alpha-Synuclein. *Angew. Chem., Int. Ed. 55*, 7374−7378.
(38) Molnar, I., and Horvath, C. (1976) Reverse-phase chromatography of polar biological substances: separation of catechol compounds by high-performance liquid chromatography. *Clin. Chem. 22*, 1497−1502.
(39) Masuda, M., Dohmae, N., Nonaka, T., Oikawa, T., Hisanaga, S. I., Goedert, M., and Hasegawa, M. (2006) Cysteine misincorporation in bacterially expressed human alpha-synuclein. *FEBS Lett. 580*, 1775−1779.
(40) Maltsev, A. S., Ying, J., and Bax, A. (2012) Impact of N-terminal acetylation of alpha-synuclein on its random coil and lipid binding properties. *Biochemistry 51*, 5004−5013.

DOI: 10.1021/acs.biochem.7b01164
Biochemistry 2018, 57, 1462−1474

(41) Kornienko, A., and La Clair, J. J. (2017) Covalent modification of biological targets with natural products through Paal-Knorr pyrrole formation. *Nat. Prod. Rep. 34*, 1051−1060.
(42) Frank, H., Woiwode, W., Nicholson, G., and Bayer, E. (1981) Determination of the rate of acidic catalyzed racemization of protein amino acids. *Liebigs Annalen der Chemie 1981*, 354−365.
(43) Balla, J., Kiss, T., and Jameson, R. F. (1992) Copper(II)-Catalyzed Oxidation of Catechol by Molecular-Oxygen in Aqueous-Solution. *Inorg. Chem. 31*, 58−62.
(44) Anderson, D. G., Mariappan, S. V., Buettner, G. R., and Doorn, J. A. (2011) Oxidation of 3,4-dihydroxyphenylacetaldehyde, a toxic dopaminergic metabolite, to a semiquinone radical and an ortho-quinone. *J. Biol. Chem. 286*, 26978−26986.
(45) Bonnett, R., and North, S. A. (1981) The Chemistry of the Isoindoles. *Adv. Heterocycl. Chem. 29*, 341−399.
(46) Lee, J. H., Ying, J., and Bax, A. (2016) Nuclear Magnetic Resonance Observation of alpha-Synuclein Membrane Interaction by Monitoring the Acetylation Reactivity of Its Lysine Side Chains. *Biochemistry 55*, 4949−4959.
(47) Brownlee, M., Vlassara, H., and Cerami, A. (1984) Non-enzymatic glycosylation and the pathogenesis of diabetic complications. *Ann. Intern. Med. 101*, 527−537.

DOI: 10.1021/acs.biochem.7b01164
Biochemistry 2018, 57, 1462−1474